Published in final edited form as:
Cell Rep. 2014 May 22; 7(4): 982–988. doi:10.1016/j.celrep.2014.04.020.

Calcineurin is universally involved in vesicle endocytosis at neuronal and non-neuronal secretory cells

Xin-Sheng Wu[*], **Zhen Zhang**[*], **Wei-Dong Zhao**[*], **Dongsheng Wang**, **Fujun Luo**, and **Ling-Gang Wu**
National Institute of Neurological Disorders and Stroke, Bethesda, MD 20892

Abstract

Calcium influx triggers and accelerates endocytosis in nerve terminals and non-neuronal secretory cells. Whether calcium/calmodulin-activated calcineurin, which dephosphorylates endocytic proteins, mediates this process is highly controversial for different cell types, developmental stages, and endocytic forms. At three preparations where controversies arose, including large calyx-type synapses, conventional cerebellar synapses and neuroendocrine chromaffin cells containing large dense-core vesicles, we reported that calcineurin gene knockout consistently slowed down endocytosis, regardless of cell types, developmental stages, or endocytic forms (rapid or slow). In contrast, calcineurin and calmodulin blockers slowed down endocytosis at relatively small calcium influx, but did not inhibit endocytosis at large calcium influx, resulting in false-negative results. These results suggest that calcineurin is universally involved in endocytosis. They may also help explain the controversies in pharmacological studies. We therefore suggest including calcineurin as a key player in mediating calcium-triggered and -accelerated vesicle endocytosis.

Introduction

Accumulated studies suggest that calcium influx triggers and accelerates endocytosis, which recycles vesicles at nerve terminals and non-neuronal secretory cells (Wu et al., 2014). Calcineurin (CaN), a calcium/calmodulin-activated phosphatase that dephosphorylates endocytosis proteins, has long been suspected as mediating this calcium-regulated process (Marks and McMahon, 1998; Cousin and Robinson, 2001). However, two decades of studies are controversial. It has been suggested that CaN blockers may or may not inhibit endocytosis at chromaffin cells (Artalejo et al., 1996; Engisch and Nowycky, 1998; Chan and Smith, 2001); do not block endocytosis at Drosophila neuromuscular junctions (Kuromi

Corresponding author: Ling-Gang Wu, wul@ninds.nih.gov.
*equal contribution

Author contributions: Xin-Sheng Wu, Zhen Zhang and Wei-Dong Zhao performed experiments in calyces, cerebellar synapses and chromaffin cells, respectively. Dongsheng Wang did the western blot. Fujun Luo participated in calyx recordings. Xin-Sheng Wu, Zhen Zhang, and Ling-Gang Wu designed experiments and wrote the paper.

et al., 1997); inhibit bulk endocytosis, but not clathrin-dependent slow endocytosis at cerebellar synapses (Clayton et al., 2009); and inhibit slow clathrin-dependent endocytosis at hippocampal synapses (Sun et al., 2010). It has been implicated that CaN blockers inhibit endocytosis at synaptosomes in adult, but not juvenile animals (Smillie et al., 2005), suggesting a developmental switch of CaN. In contrast, CaN blockers inhibit endocytosis at immature, but not mature calyces, suggesting an opposite developmental switch (Yamashita et al., 2010). The conflict at the same preparation, different preparations, different developmental stages, and different endocytic forms seriously questions whether CaN is universally involved in endocytosis. CaN is thus not considered a key player like clathrin and dynamin in vesicle endocytosis (Dittman and Ryan, 2009; Saheki and De Camilli, 2012; Wu et al., 2014).

Here we report that CaN knockout inhibited endocytosis regardless of the endocytic (rapid and slow) forms or developmental stages in three preparations where the controversy arose, including large calyx-type synapses, small conventional cerebellar synapses and endocrine chromaffin cells. Calcineurin and calmodulin blockers may produce false-negative results, because their effects were calcium-dependent, which may explain the conflicting results of CaN. These results established CaN as a key endocytic player in secretory cells and may largely end the debate on whether calcineurin is involved in endocytosis.

Results

Calcineurin involvement in rapid and slow endocytosis at immature and mature calyces

CaN is composed of a catalytic A (CaN_A) and a regulatory B subunit. CaN_A has α and β isoforms in neurons. $CaN_{A\alpha}$ knockout and CaN blockers inhibit endocytosis at P7-10 immature calyces (Sun et al., 2010), whereas CaN blockers fail to inhibit endocytosis at P13-14 mature calyces, leading to a suggestion that the endocytosis calcium sensor switches from CaN to an unknown one as synapses mature (Yamashita et al., 2010). Here we re-addressed this issue using $CaN_{A\alpha}^{-/-}$ mice.

We induced slow clathrin-dependent endocytosis with a 20 ms depolarization ($depol_{20ms}$) from -80 mV to +10 mV (Fig. 1A) (Wu et al., 2009; Hosoi et al., 2009), and rapid endocytosis with 10 $depol_{20ms}$ at 10 Hz ($depol_{20msx10}$, Fig. 1B). These two stimuli are equivalent to 10-50 and 200 action potentials at 100 Hz in inducing slow and rapid endocytosis, respectively (Fig. S1) (Wu et al., 2005; Wu et al., 2009). In P13-14 wild-type littermates, $depol_{20ms}$ induced a capacitance jump (ΔCm) of 480 ± 28 fF, followed by a slow mono-exponential decay with a τ of 17 ± 1 s and an initial decay rate ($Rate_{decay}$) of 28 ± 2 fF/s (n = 12, Fig. 1A). $Depol_{20msX10}$ induced a ΔCm of 1378 ± 78 fF, followed by a bi-exponential decay with τ of 2.0 ± 0.1 s (30 ± 4%) and 19.7 ± 1.9 s (n = 12), and a $Rate_{decay}$ of 229 ± 27 fF/s (n = 12, Fig. 1B) that reflects mostly (> 80%) the rapid endocytic component (Wu et al., 2009; Sun et al., 2010). We used mostly $Rate_{decay}$ for statistics, because τ was often too slow to estimate in knockout mice.

Compared to wild-type, $Rate_{decay}$, but not ICa or ΔCm ($p > 0.3$), induced by $depol_{20ms}$ and $depol_{20msX10}$ was reduced in P13-14 $CaN_{A\alpha}^{-/-}$ mice ($p < 0.01$, Fig. 1A-C), similar to that observed in P7-10 $CaN_{A\alpha}^{-/-}$ mice (Fig. 1D, Sun et al., 2010). The inhibition of slow and

rapid endocytosis was also observed after 20 or 200 action potential-equivalent stimuli (APe, 1 ms from -80 to +7 mV) (Xu and Wu, 2005) at 100 Hz in P13-14 $CaN_{A\alpha}^{-/-}$ mice (Fig. S1). Thus, CaN is involved in slow and rapid endocytosis as calyces mature from P7 to P14.

Calcineurin and calmodulin blockers' efficiency depends on calcium buffer concentration and calcium influx

As in the previous study (Yamashita et al., 2010), CaN auto-inhibitory peptide ($CaN_{457-482}$, 200 μM in the pipette) did not reduce $Rate_{decay}$ after $depol_{20ms}$ and $depol_{20msX10}$ with a pipette containing 0.05 mM BAPTA at P13-14 rat calyces (Fig. 2A-C). However, with 2.5 mM EGTA in the pipette, $CaN_{457-482}$ significantly reduced $Rate_{decay}$ without affecting ICa or ΔCm at P13-14 rat calyces (Fig. 2D-F). This reduction depended on the EGTA concentration, because as the EGTA concentration increased from 0 (0.05 mM BAPTA), to 0.5, 1.25, and 2.5 mM, the $Rate_{decay}$ decreased in the presence of $CaN_{457-482}$, but did not decrease in the absence of $CaN_{457-482}$ (Fig. 2G). The result that 2.5 mM EGTA did not affect $Rate_{decay}$ in P13-14 mice (Fig. 2G, right, $p = 0.14$) is consistent with a previous study (Yamashita et al., 2010). Similar to Fig. 2D-G, after 20 APe at 100 Hz in P13-14 calyces, $CaN_{457-482}$ did not reduce $Rate_{decay}$ in control (0.05 mM BAPTA), but significantly reduce $Rate_{decay}$ in the presence of 2.5 mM EGTA (Fig. S2). We also found that a calmodulin blocker, the myosin light chain kinase peptide (20 μM), did not reduce $Rate_{decay}$ in pipettes containing 0.05 mM BAPTA (Fig. S3A-C), but reduced $Rate_{decay}$ in pipettes containing 2.5 mM EGTA at P13-14 rat calyces (Fig. S3D-F). These pharmacological results were consistent with the results in $CaN_{A\alpha}^{-/-}$ mice. We conclude that the efficiency of CaN and calmodulin blockers depends on calcium buffer concentrations, which explains the lack of effects of CaN and calmodulin blockers in the presence of 0.5 mM EGTA (Yamashita et al., 2010).

Even at P7-10 rat calyces where CaN blockers were effective with 0.05 mM BAPTA or 0.5 mM EGTA (Sun et al., 2010; Yamashita et al., 2010), the CaN blocker cyclosporine A inhibited endocytosis induced by 20 APe, $depol_{20ms}$, and $depol_{20msX10}$, but not by 10 pulses of 50 ms depolarization at 10 Hz that caused very large calcium influx (Fig. S4). Thus, the effects of CaN inhibitors depend on calcium influx, which may help resolve the CaN conflict.

Calcineurin is involved in slow endocytosis at cerebellar synapses

At cerebellar synapses, CaN is not considered to be involved in slow clathrin-dependent endocytosis (Clayton et al., 2009). To re-address this issue, mouse cerebellar granule cell culture was transfected with synaptophysin-pHluroin2X (SypH2X) for endocytosis imaging (Zhu et al., 2009). In wild-type, a 10 s action potential train at 20 Hz ($Train_{20Hz}$) induced a fluorescence increase (ΔF) of 48 ± 10% (of the baseline intensity), followed by a mono-exponential decay with a τ of 14.8 ± 1.8 s (n = 4, Fig. 3A). A 10 s train at 40 Hz ($Train_{40Hz}$) induced a larger ΔF of 109 ± 20%, followed by a slower mono-exponential decay with a τ of 33.7 ± 4.1 s (n = 4, Fig. 3B), likely due to small, global calcium increase that inhibits endocytosis (Wu and Wu, 2014).

In $CaN_{A\alpha}^{-/-}$ cerebellar cultures, $Train_{20Hz}$ induced a ΔF (12 ± 1%, n = 8) smaller than the wild-type ($p < 0.01$, Fig. 3A). The fluorescence increase did not decay (Fig. 3A), suggesting impairment of endocytosis. $Train_{40Hz}$ induced a ΔF (54 ± 8%, n = 5, Fig. 3B) smaller than the wild-type after $Train_{40Hz}$ ($p < 0.01$, Fig. 3B), but similar to the wild-type after $Train_{20Hz}$ (Fig. 3A). The decay τ (136 ± 44 s, n = 5, Fig. 3B) was slower than the wild-type after $Train_{40Hz}$ ($p < 0.05$, Fig. 3B) or $Train_{20Hz}$ ($p < 0.01$, Fig. 3A). Thus, the slower endocytosis in $CaN_{A\alpha}^{-/-}$ culture was not due to decreased ΔF (compare Fig. 3B red trace with Fig. 3 A black trace). This conclusion was further supported by the finding that decreasing exocytosis in control does not slow down endocytosis (Fig. 3A-B) (Wu and Betz, 1996; Wu et al., 2005; Sankaranarayanan and Ryan, 2000).

A shRNA knocks down $CaN_{A\alpha}$ and reduce calcium influx at hippocampal synapses (Kim and Ryan, 2013). Here, the slower endocytosis in $CaN_{A\alpha}^{-/-}$ mice is not due to reduction of calcium influx, because $CaN_{A\alpha}$ knockout did not affect the fluorescence (baseline, increase, and fractional increase) of the calcium indicator fluo2 loaded at boutons during $Train_{20Hz}$ (Figs. 3C, S1E), or ICa at calyces (Fig. 1) and chromaffin cells described later. It is neither caused by changed expression of main endocytic proteins, because expression of clathrin, dynamin, AP2 and endophilin were not affected by $CaN_{A\alpha}$ knockout (Fig. 3D). We conclude that CaN is involved in slow endocytosis at cerebellar synapses.

Calcineurin involvement in endocytosis at chromaffin cells

In adrenal chromaffin cells, conflicting results regarding whether calcineurin blockers inhibit endocytosis were reported (Artalejo et al., 1996; Engisch and Nowycky, 1998; Chan and Smith, 2001). Here we determined whether $CaN_{A\alpha}$ knockout inhibits endocytosis. In wild-type mice, 1 s depolarization (from -80 to +10 mV) induced an ICa of 385 ± 65 pA and a ΔCm of 546 ± 83 fF, followed by a mono-exponential decay with a τ of 11 ± 3.3 s and a $Rate_{decay}$ of 55 ± 11.1 fF/s (n = 17, Fig. 4A-B). In $CaN_{A\alpha}^{-/-}$ mice, 1 s depolarization induced an ICa (339 ± 39 pA) and a ΔCm (551 ± 46 fF, n = 25) similar to wild-type, but a significantly prolonged capacitance decay and a smaller $Rate_{decay}$ (29.6 ± 4.2 fF/s, n = 25, $p < 0.05$, Fig. 4A-B), suggesting CaN involvement in endocytosis of chromaffin cells.

Discussion

We found the involvement of CaN in rapid and slow endocytosis in three preparations at various developmental stages and stimuli (Figs. 1, 3, 4), suggesting universal involvement of CaN in endocytosis at neurons and non-neuronal secretory cells. Given the overwhelming evidence that calcium influx triggers and/or accelerates various forms of endocytosis, including rapid, slow, and bulk endocytosis in nerve terminals and endocrine cells (reviewed in Wu et al., 2014), CaN may serve as a universal calcium sensor mediating the calcium-triggered and/or calcium-accelerated endocytosis. We also found that the efficiency of CaN and calmodulin blockers in inhibiting endocytosis depended on calcium, which may result in false-negative results at low calcium buffers or large calcium influx (Figs. 2, S2-4). These findings may help resolve the large scale CaN controversy, and establish CaN as a key endocytic player in secretory cells regardless of the cell types, developmental stages, and endocytic forms.

Calmodulin and CaN blockers inhibit endocytosis at immature, but not mature calyces dialyzed with 0.5 mM EGTA, which was interpreted as a developmental switch of the endocytic calcium sensor from calmodulin/CaN to an unknown one (Yamashita et al., 2010). This interpretation needs to be reconsidered, because the effects of CaN and calmodulin blockers depended on calcium buffer concentration and calcium influx (Figs. 2, S2-4). These blockers were ineffective at 0.5 mM EGTA, but effective at higher EGTA concentrations in mature calyces (Figs. 2, S2-3). Furthermore, $CaN_{A\alpha}$ knockout inhibited endocytosis at both mature and immature calyces (Fig. 1). Thus, CaN and calmodulin are involved in endocytosis at both mature and immature calyces.

EGTA inhibits exo- and endocytosis at immature, but not mature calyces, suggesting a tighter coupling between calcium channels and exo- and endocytosis at mature calyces (Wang et al., 2008; Yamashita et al., 2010). A tighter coupling, likely due to a shorter distance between calcium channels and the endocytic site or a lower calcium buffer concentration, may increase the calcium concentration at the endocytic site during calcium influx. The higher calcium concentration might activate the unblocked CaN and calmodulin to a larger extent to compensate for the partial block by CaN and calmodulin blockers, which may explain the apparent lack of effects of CaN and calmodulin blockers on endocytosis at P13-14 calyces dialyzed with a low concentration of calcium buffers (Figs. 2, S2-3) (Yamashita et al., 2010).

A previous implication that CaN is not involved in clathrin-dependent endocytosis at cerebellar synapses is mainly supported by two observations (Clayton et al., 2009). First, dynamin ser-774 and ser-778 dephosphorylation by CaN is undetectable at relatively low frequency (e.g., 20 Hz) firings that induce slow endocytosis. Second, overexpression of dynamin I phospho-mimetic mutant (ser-774 and ser-778 cannot be dephosphorylated by CaN) blocks dye uptake into large endosomes, but not small vesicles presumably formed via clathrin-dependent endocytosis. These results do not necessarily contradict our results, because 1) dynamin dephosphorylation may occur, but below the detection limit, 2) overexpressed dynamin I phospho-mimetic mutant may not fully block, and thus exclude endogenous dynamin dephosphorylation, 3) CaN-mediated dephosphorylation of proteins other than dynamin I has not been excluded, and 4) whether blocking CaN inhibits slow endocytosis has not been tested at cerebellar synapses. We found that $CaN_{A\alpha}$ knockout impaired slow endocytosis after 20 - 40 Hz firing (Fig. 3 A-B). This finding, together with the previous finding that CaN is involved in bulk endocytosis (Clayton et al., 2009), suggests the involvement of CaN in both slow and bulk endocytosis at cerebellar synapses.

After 0.5-1 s depolarization, endocytosis detected with capacitance measurements was inhibited by CaN blockers at chromaffin cells in one (Engisch and Nowycky, 1998), but not another study (Artalejo et al., 1996). However, the lack of effects were obtained from calf chromaffin cells, where ICa was ∼700-1400 pA (shown in figures) and the mean was ∼800 pA (Artalejo et al., 1996), whereas the positive effect was observed in adult bovine chromaffin cells where ICa was ∼600-800 pA (shown in figures) and the mean (not reported) seems much smaller as we estimated from ICa charge (Engisch and Nowycky, 1998). The differences in ICa might therefore explain the differential effects of CaN blockers, given that CaN blocker efficiency depends on calcium buffer concentrations and

calcium influx (Figs. 2, S2-4). This explanation, together with our finding that $CaN_{A\alpha}$ knockout impaired endocytosis (Fig. 4), re-establishes CaN as an endocytic player in calcium-regulated endocytosis at chromaffin cells.

CaN is implied to regulate endocytosis during high, but not low frequency action potential-like stimuli at chromaffin cells (Chan and Smith, 2001). However, endocytosis is derived from the difference between exocytosis from a small cell patch (amperometric recording) and the whole-cell capacitance increase (Chan and Smith, 2001). This calculation assumes constant baseline capacitance over a long time and same release rates between a cell patch and the whole cell, both of which have not been verified. Furthermore, capacitance decay after action potential-like trains has not been reported and was too slow to measure in 40 s recording time in our hands (Chiang et al., 2014). Thus, more reliable techniques seem needed to study endocytosis induced by action potential trains in chromaffin cells.

CaN blockers inhibit FM dye release from synaptosomes (after FM dye loading) of adult, but not juvenile animals, which was interpreted as a developmental switch of the endocytosis calcium sensor from an unknown one to CaN (Smillie et al., 2005). However, synaptosomes without connecting axons may be severely damaged, and can only be stimulated with prolonged non-physiological high potassium stimulation. Endocytosis time course from synaptosomes has not been reported directly, but implicated from FM dye release, which reflects not only endocytosis, but also recycling vesicle pool size, vesicle mobilization to the readily releasable pool, release probability, calcium channels, or other mechanisms that regulate release. Thus, while the interpretation that endocytosis calcium sensor switches developmentally from an unknown one to CaN (Smillie et al., 2005) differs from our conclusion, the supporting experimental results do not directly contradict our results and can be interpreted with different scenarios.

In summary, most previous studies reporting no effects of CaN and calmodulin blockers on endocytosis might be due to strong calcium influx that reduces the efficiency of CaN and calmodulin blockers (Figs. 2, S2-4), or subjected to alternative interpretations that do not contradict our conclusion. The present work may thus resolve the long-term debate on whether CaN is involved in endocytosis and establish CaN as a universal key player for rapid and slow endocytosis in neurons and non-neuronal secretory cells. Given that CaN and calcium/calmodulin that activates calcineurin are involved in bulk endocytosis in nerve terminals (Clayton et al., 2009; Wu et al., 2009), we suggest CaN as a universal player for rapid, slow, and bulk endocytosis.

What is the downstream target of CaN? Among many endocytic proteins that can be dephosphorylated by CaN, dynamin is considered a downstream target (Cheung and Cousin, 2013; Armbruster et al., 2013). Since endocytosis was not fully blocked by $CaN_{A\alpha}$ knockout (Figs. 1, 3, 4), $CaN_{A\beta}$ or other calcium-sensing proteins might also participate in mediating calcium-regulated endocytosis (Poskanzer et al., 2006; Nicholson-Tomishima and Ryan, 2004; Yao et al., 2011). It would be of interest to address this issue in the future.

Methods

Animals

$CaN_{A\alpha}^{-/-}$ mice were obtained by heterozygous breeding using standard mouse husbandry procedures. Mouse genotypes were determined by PCR reaction (Sun et al., 2010).

Calyx recordings

Parasagittal brainstem slices (200 μm thick) containing the medial nucleus of the trapezoid body were prepared from 7 - 14 days old male or female mice using a vibratome. Whole-cell capacitance measurements were made with the EPC-9 amplifier (Sun and Wu, 2001; Sun et al., 2004). We pharmacologically isolated Ca^{2+} currents with a bath solution (~22 - 24 °C) containing (in mM): 105 NaCl, 20 TEA-Cl, 2.5 KCl, 1 $MgCl_2$, 2 $CaCl_2$, 25 $NaHCO_3$, 1.25 NaH_2PO_4, 25 glucose, 0.4 ascorbic acid, 3 *myo*-inositol, 2 sodium pyruvate, 0.001 tetrodotoxin (TTX), 0.1 3,4-diaminopyridine, pH 7.4 when bubbled with 95% O_2 and 5% CO_2. The presynaptic pipette contained (in mM): 125 Cs-gluconate, 20 CsCl, 4 MgATP, 10 Na_2-phosphocreatine, 0.3 GTP, 10 HEPES, 0.05 BAPTA, pH 7.2, adjusted with CsOH. $CaN_{457\text{-}482}$ and scrambled $CaN_{457\text{-}482}$ were purchased from Calbiochem, and GenScript USA Inc., respectively. MLCK was purchased from EMD Chemicals. Other reagents were purchased from Sigma.

Cerebellar granule cell culture and imaging

Cerebellum (P8 mice) was dissected, dissociated, and plated on Poly-D-lysine coated glass coverslips. Cells were maintained (37°C) in a 5% CO_2 humidified incubator with a medium consisting of MEM, 25 mM KCl, 10% fetal bovine serum, 2 mM glutamine, 100 U/ml penicillin and 100 μg/ml streptomycin (Invitrogen). At 1, 3 and 4 days after plating, we added 10 μM cytosine β-D-arabinofuranoside, 25 mM glucose, and transfected SypH2X to the culture via lipofectamine-mediated gene transfer, respectively. Cells were used 5 - 8 days after transfection.

Coverslips containing cultured cells were mounted in a chamber, where a 1 ms, 20 mA pulse applied via platinum electrodes evoked an action potential (Sun et al., 2010). The bath solution (~22 - 24 °C) contained (in mM): 119 NaCl, 2.5 KCl, 2 $CaCl_2$, 2 $MgCl_2$, 25 HEPES (buffered to pH 7.4), 30 glucose, 0.01 6-cyano-7-nitroquinoxaline-2, 3-dione (CNQX) and 0.05 d, l-2-amino-5-phosphonovaleric acid (AP-5).

SypH2X or fluo2 images were acquired at 1-2 Hz with Nikon A1 confocal microscope. Varicosities (1.5 μm × 1.5 μm) responded to stimulation were analyzed. Each data group was obtained from ≥ 3 batches of cultures. Fluo2 was excited at 488 nm. Its fluorescence at 505 - 530 nm was collected.

Western blot

Mouse brains were homogenized in the modified RIPA buffer containing protease inhibitors (Thermo Scientific). Equal amounts of proteins from wild-type and $CaN_{A\alpha}^{-/-}$ mice, determined by BCA protein assay, were loaded onto SDS-PAGE gel and immunoblotted using antibodies against $CaN_{A\alpha}$ (1:200, Santa Cruz Biotechnology), clathrin (1:1,000, BD

Bioscience), dynamin (1:1,000, BD Bioscience), AP2 (1:100, Thermo Scientific), endophilin (1:200, Invitrogen) and actin (1: 400, Abcam).

Primary chromaffin cell culture and electrophysiology

We prepared primary chromaffin cell culture as described previously (Fulop et al., 2005). 2-month-old mouse adrenal glands were immersed in a dissociation solution containing (mM): Na-glutamate, 80; NaCl, 55; KCl, 6; $MgCl_2$, 1; HEPES, 10; pH 7.0 adjusted with NaOH. Medulla was dissected and digested in the dissociation solution with papain (30 U/ml), BSA (0.5 mg/ml) and DTT (0.1 mM, (37°C, 10 min), and further digested with collagenase F (3 U/ml), BSA (0.5 mg/ml) and $CaCl_2$ (0.1 mM, 37°C, 10 min). The digested medulla was minced in DMEM medium (Invitrogen) containing 10% fetal bovine serum and then centrifuged (2000 rpm, 2 min). Final cell pellet was resuspended in pre-warmed DMEM medium and plated onto poly-L-lysine (0.005 % w/v) and laminin (4 μg/ml) coated glass coverslips. Cells were incubated at 37°C with 8% CO_2 and used within 4 days.

At room temperature (22 - 24°C), whole-cell voltage-clamp and capacitance recordings were performed with an EPC-10 amplifier (holding potential: -80 mV; sinusoidal frequency: 1000-1500 Hz; peak-to-peak voltage ≤ 50 mV). The bath solution contained (in mM) 125 NaCl, 10 glucose, 10 HEPES, 5 $CaCl_2$, 1 $MgCl_2$, 4.5 KCl, 0.001 TTX and 20 TEA, pH 7.3 adjusted with NaOH. The pipette (3 – 5 MΩ) solution contained (in mM) 130 Cs-glutamate, 0.5 Cs-EGTA, 12 NaCl, 30 HEPES, 1 $MgCl_2$, 2 ATP, and 0.5 GTP, pH 7.2 adjusted with CsOH. These solutions pharmacologically isolated calcium currents.

Data collection and analysis

To avoid rundown, calyces were measured within 10 min after break in (Xu et al., 2008), and chromaffin cells were measured within 2 min after break in (first stimulus only). $Rate_{decay}$ at calyces was measured within 4 s after $depol_{20ms}$ or 20 APe at 100 Hz that induced slow endocytosis, but within 1 - 1.5 s after $depol_{20msX10}$ or 200 APe at 100 Hz that induced rapid endocytosis. We used $depol_{20msX10}$ to induce rapid endocytosis, because the $Rate_{decay}$ after $depol_{20msX10}$ reflected mostly (∼80%) the rapid component of endocytosis, as described previously (Wu et al., 2009). For chromaffin cells, $Rate_{decay}$ was measured within 4 - 6 s after depolarization.

The statistical test was t-test. Means were presented as ± s.e.m.

Supplementary Material

Refer to Web version on PubMed Central for supplementary material.

Acknowledgments

This work was supported by the National Institute of Neurological Disorders and Stroke Intramural Research Program. We thank Drs. Jonathan G. Seidman (Harvard Medical School) and Jennifer L. Gooch (Emory University School of Medicine) for providing calcineurin $A_\alpha^{+/-}$ mice, and Dr Yong-Ling Zhu (Northwestern University) for providing SypH2X construct. We thank Dr. Edaeni Hamid for commenting the manuscript.

Reference List

Armbruster M, Messa M, Ferguson SM, De CP, Ryan TA. Dynamin phosphorylation controls optimization of endocytosis for brief action potential bursts. Elife. 2013; 2:e00845. [PubMed: 23908769]

Artalejo CR, Elhamdani A, Palfrey HC. Calmodulin is the divalent cation receptor for rapid endocytosis, but not exocytosis, in adrenal chromaffin cells. Neuron. 1996; 16:195–205. [PubMed: 8562084]

Chan SA, Smith C. Physiological stimuli evoke two forms of endocytosis in bovine chromaffin cells. J Physiol. 2001; 537:871–885. [PubMed: 11744761]

Cheung G, Cousin MA. Synaptic vesicle generation from activity-dependent bulk endosomes requires calcium and calcineurin. J Neurosci. 2013; 33:3370–3379. [PubMed: 23426665]

Chiang HC, Shin W, Zhao WD, Hamid E, Sheng J, Baydyuk M, Wen PJ, Jin A, Momboisse F, Wu LG. Post-fusion structural changes and their roles in exocytosis and endocytosis of dense-core vesicles. Nat Commun. 2014; 5:3356. [PubMed: 24561832]

Clayton EL, Anggono V, Smillie KJ, Chau N, Robinson PJ, Cousin MA. The phospho-dependent dynamin-syndapin interaction triggers activity-dependent bulk endocytosis of synaptic vesicles. J Neurosci. 2009; 29:7706–7717. [PubMed: 19535582]

Cousin MA, Robinson PJ. The dephosphins: dephosphorylation by calcineurin triggers synaptic vesicle endocytosis. Trends Neurosci. 2001; 24:659–665. [PubMed: 11672811]

Dittman J, Ryan TA. Molecular Circuitry of Endocytosis at Nerve Terminals. Annu Rev Cell Dev Biol. 2009; 25:133–160. [PubMed: 19575674]

Engisch KL, Nowycky MC. Compensatory and excess retrieval: two types of endocytosis following single step depolarizations in bovine adrenal chromaffin cells. J Physiol. 1998; 506(Pt 3):591–608. [PubMed: 9503324]

Fulop T, Radabaugh S, Smith C. Activity-dependent differential transmitter release in mouse adrenal chromaffin cells. J Neurosci. 2005; 25:7324–7332. [PubMed: 16093382]

Hosoi N, Holt M, Sakaba T. Calcium dependence of exo- and endocytotic coupling at a glutamatergic synapse. Neuron. 2009; 63:216–229. [PubMed: 19640480]

Kim SH, Ryan TA. Balance of Calcineurin Aalpha and CDK5 Activities Sets Release Probability at Nerve Terminals. J Neurosci. 2013; 33:8937–8950. [PubMed: 23699505]

Kuromi H, Yoshihara M, Kidokoro Y. An inhibitory role of calcineurin in endocytosis of synaptic vesicles at nerve terminals of Drosophila larvae. Neurosci Res. 1997; 27:101–113. [PubMed: 9100252]

Marks B, McMahon HT. Calcium triggers calcineurin-dependent synaptic vesicle recycling in mammalian nerve terminals. Curr Biol. 1998; 8:740–749. [PubMed: 9651678]

Nicholson-Tomishima K, Ryan TA. Kinetic efficiency of endocytosis at mammalian CNS synapses requires synaptotagmin I. Proc Natl Acad Sci U S A. 2004; 101:16648–16652. [PubMed: 15492212]

Poskanzer KE, Fetter RD, Davis GW. Discrete residues in the c(2)b domain of synaptotagmin I independently specify endocytic rate and synaptic vesicle size. Neuron. 2006; 50:49–62. [PubMed: 16600855]

Saheki Y, De Camilli P. Synaptic vesicle endocytosis. Cold Spring Harb. Perspect Biol. 2012; 4:a005645.

Sankaranarayanan S, Ryan TA. Real-time measurements of vesicle-SNARE recycling in synapses of the central nervous system. Nat Cell Biol. 2000; 2:197–204. [PubMed: 10783237]

Smillie KJ, Evans GJ, Cousin MA. Developmental change in the calcium sensor for synaptic vesicle endocytosis in central nerve terminals. J Neurochem. 2005; 94:452–458. [PubMed: 15998295]

Sun JY, Wu LG. Fast kinetics of exocytosis revealed by simultaneous measurements of presynaptic capacitance and postsynatpic currents at a central synapse. Neuron. 2001; 30:171–182. [PubMed: 11343653]

Sun JY, Wu XS, Wu W, Jin SX, Dondzillo A, Wu LG. Capacitance measurements at the calyx of Held in the medial nucleus of the trapezoid body. J Neurosci Methods. 2004; 134:121–131. [PubMed: 15003378]

Sun T, Wu XS, Xu J, McNeil BD, Pang ZP, Yang W, Bai L, Qadri S, Molkentin JD, Yue DT, Wu LG. The role of calcium/calmodulin-activated calcineurin in rapid and slow endocytosis at central synapses. J Neurosci. 2010; 30:11838–11847. [PubMed: 20810903]

Wang LY, Neher E, Taschenberger H. Synaptic vesicles in mature calyx of Held synapses sense higher nanodomain calcium concentrations during action potential-evoked glutamate release. J Neurosci. 2008; 28:14450–14458. [PubMed: 19118179]

Wu LG, Betz WJ. Nerve activity but not intracellular calcium determines the time course of endocytosis at the frog neuromuscular junction. Neuron. 1996; 17:769–779. [PubMed: 8893033]

Wu LG, Hamid E, Shin W, Chiang HC. Exocytosis and Endocytosis: Modes, Function, and Coupling Mechanisms. Annu Rev Physiol. 2014; 76 in press.

Wu W, Xu J, Wu XS, Wu LG. Activity-dependent acceleration of endocytosis at a central synapse. J Neurosci. 2005; 25:11676–11683. [PubMed: 16354926]

Wu XS, McNeil BD, Xu J, Fan J, Xue L, Melicoff E, Adachi R, Bai L, Wu LG. Ca^{2+} and calmodulin initiate all forms of endocytosis during depolarization at a nerve terminal. Nat Neurosci. 2009; 12:1003–1010. [PubMed: 19633667]

Wu XS, Wu LG. The yin and yang of calcium effects on synaptic vesicle endocytosis. J Neurosci. 2014; 34:2652–2659. [PubMed: 24523554]

Xu J, McNeil B, Wu W, Nees D, Bai L, Wu LG. GTP-independent rapid and slow endocytosis at a central synapse. Nat Neurosci. 2008; 11:45–53. [PubMed: 18066059]

Xu J, Wu LG. The decrease in the presynaptic calcium current is a major cause of short-term depression at a calyx-type synapse. Neuron. 2005; 46:633–645. [PubMed: 15944131]

Yamashita T, Eguchi K, Saitoh N, Von Gersdorff H, Takahashi T. Developmental shift to a mechanism of synaptic vesicle endocytosis requiring nanodomain Ca^{2+} Nat Neurosci. 2010; 13:838–844. [PubMed: 20562869]

Yao J, Kwon SE, Gaffaney JD, Dunning FM, Chapman ER. Uncoupling the roles of synaptotagmin I during endo- and exocytosis of synaptic vesicles. Nat Neurosci. 2011; 15:243–249. [PubMed: 22197832]

Zhu Y, Xu J, Heinemann SF. Two pathways of synaptic vesicle retrieval revealed by single-vesicle imaging. Neuron. 2009; 61:397–411. [PubMed: 19217377]

Highlights

- Calcineurin is involved in rapid and slow endocytosis at synapses and endocrine cells
- Calcineurin is involved in endocytosis in both mature and immature synapses
- Calcineurin and calmodulin blockers' effect on endocytosis depends on calcium influx
- Resolve the debate on whether calcineurin is universally involved in endocytosis

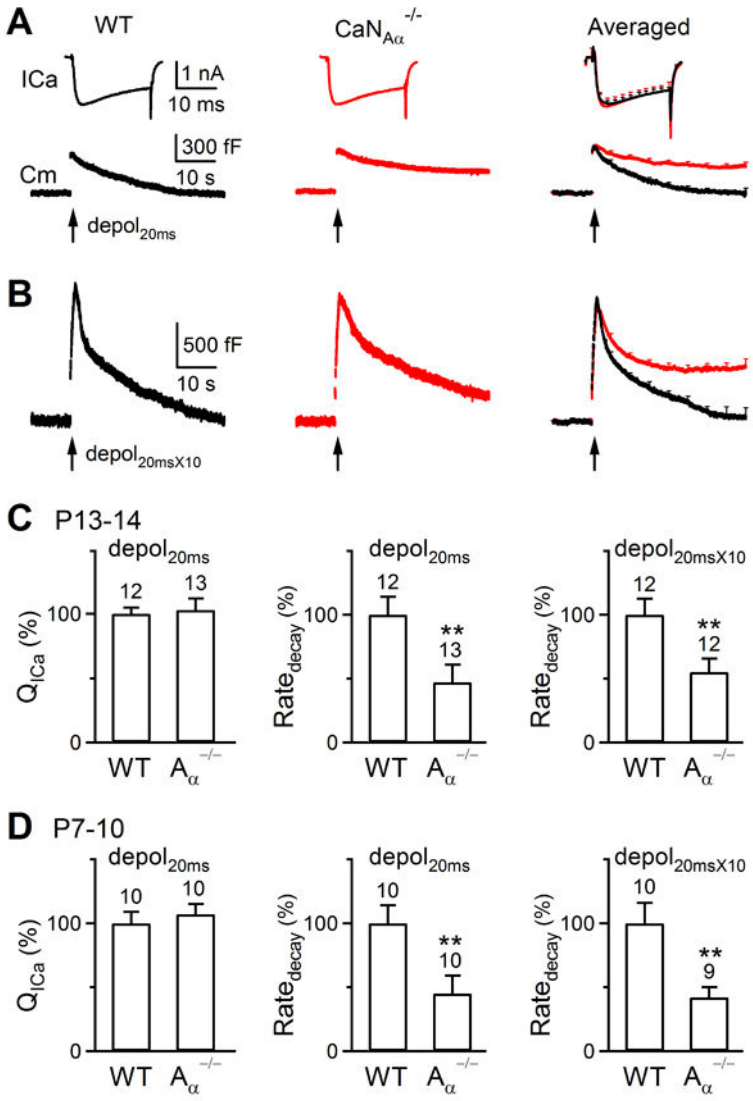

Figure 1. CaN$_{A\alpha}$ knockout inhibits endocytosis at calyces

(A) Sampled (left and middle) and averaged (right, mean + s.e.m.) ICa and Cm induced by depol$_{20ms}$ (arrow) from P13-14 wild-type (WT, black, 12 calyces) and CaN$_{A\alpha}^{-/-}$ mice (red, 13 calyces).

(B) Sampled and averaged Cm induced by depol$_{20msX10}$ (arrow) from P13-14 WT (12 calyces) and CaN$_{A\alpha}^{-/-}$ (12 calyces) mice.

(C-D) QICa and Rate$_{decay}$ induced by depol$_{20ms}$ and Rate$_{decay}$ induced by depol$_{20msX10}$ in WT and CaN$_{A\alpha}^{-/-}$ mice in P13-14 (C) or P7-10 calyces (D, data from Sun et al., 2010). **: $p<0.01$. Data were normalized to the mean of the control (WT) group and the calyx number was labeled above the bar (applies to all bar graphs).

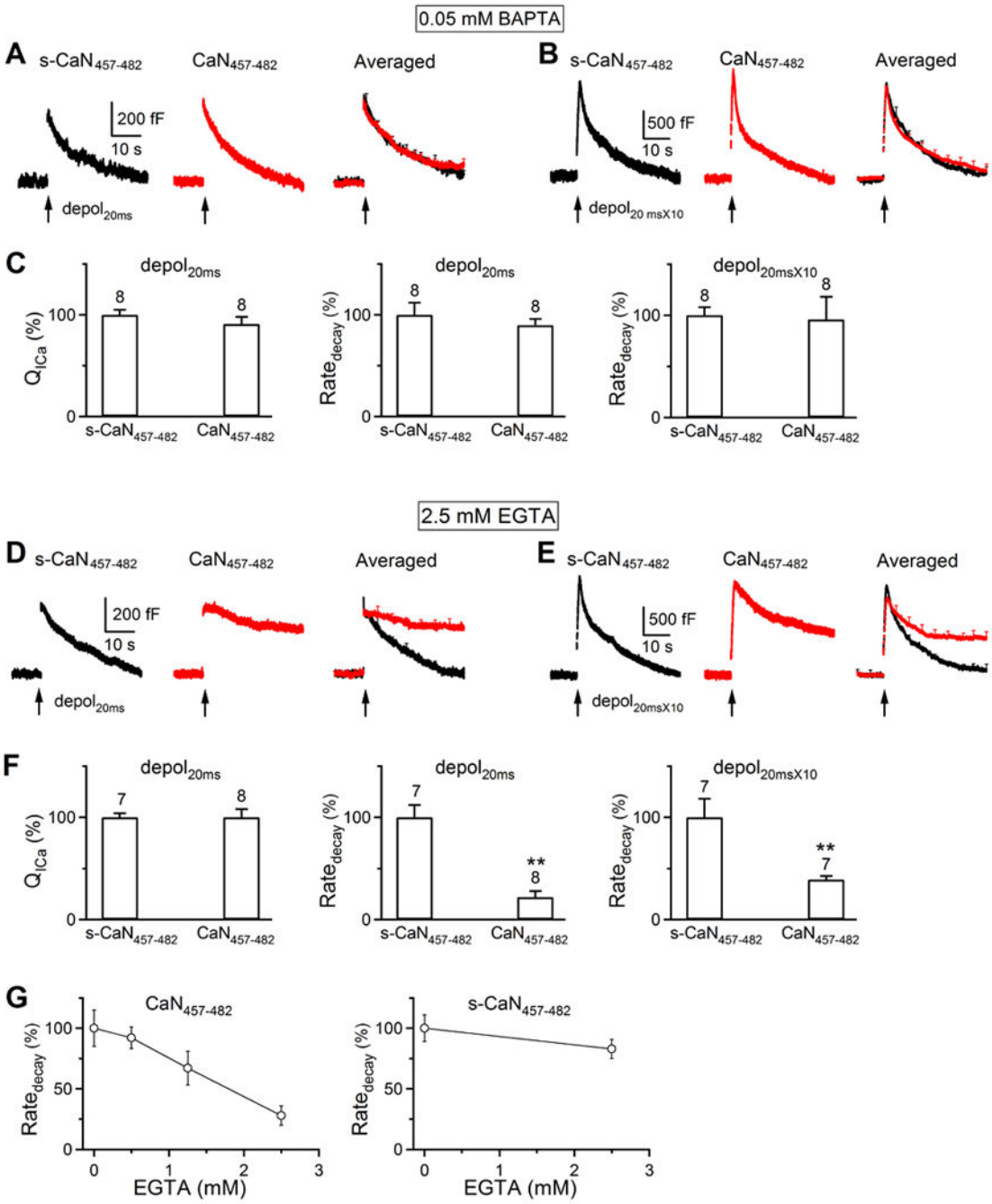

Figure 2. The inhibition of endocytosis by $CaN_{457-482}$ depends on the calcium buffer concentration at P13-14 rat calyces

(A) Sampled (left and middle) and averaged (right, mean + s.e.m) Cm changes induced by $depol_{20ms}$ with a pipette containing 0.05 mM BAPTA and either scrambled $CaN_{457-482}$ (s-$CaN_{457-482}$, 200 μM, control, black, n = 8) or $CaN_{457-482}$ (200 μM, red, n = 8) in P13-14 rat calyces (P13-14 applies to A-G).

(B) Similar to A, except that the stimulus was $depol_{20msX10}$. s-$CaN_{457-482}$, n = 8; $CaN_{457-482}$, n = 8.

(C) QICa and $Rate_{decay}$ induced by $depol_{20ms}$ and $Rate_{decay}$ induced by $depol_{20msX10}$ in control (s-$CaN_{457-482}$, n = 8, black) or in the presence of $CaN_{457-482}$ (red, n = 8). In both groups, the pipette contained 0.05 mM BAPTA.

(D-F) Similar to A-C, respectively, except that 0.05 mM BAPTA was replaced with 2.5 mM EGTA in pipettes. D: s-$CaN_{457-482}$, n = 7; $CaN_{457-482}$, n = 8. E: s-$CaN_{457-482}$, n = 7; $CaN_{457-482}$, n = 7. **: $p<0.01$.

(G) $Rate_{decay}$ (mean ± s.e.m.) induced by $depol_{20ms}$ in the presence of $CaN_{457-482}$ (200 μM, left) or s-$CaN_{457-482}$ (200 μM, right) is plotted versus the pipette EGTA concentration (n = 5 - 9 calyces). Pipettes with 0 mM EGTA contained 0.05 mM BAPTA. Data are normalized to that obtained with 0 mM EGTA.

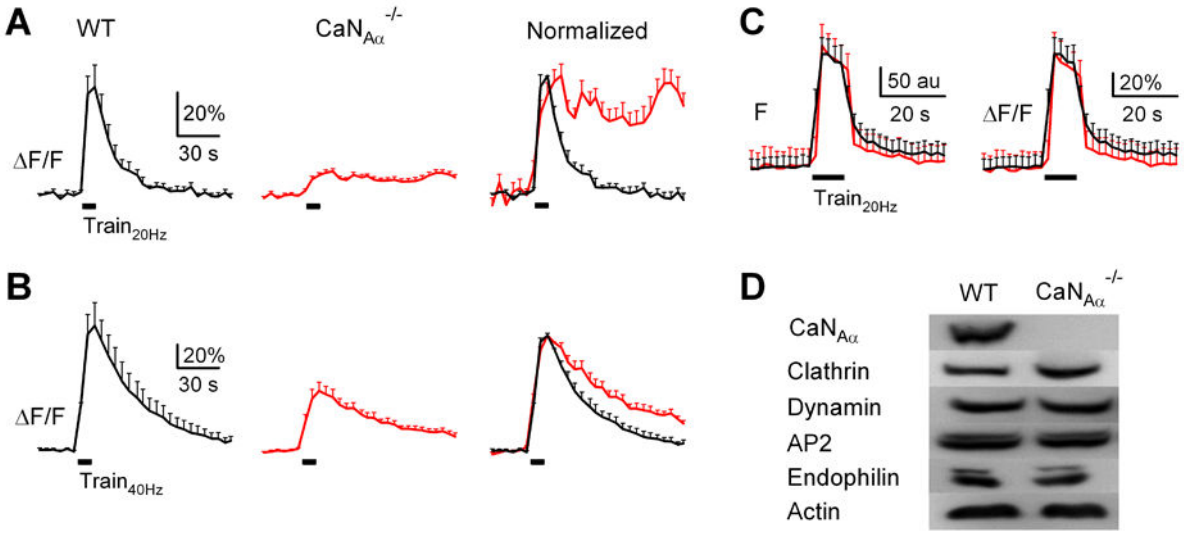

Figure 3. CaN$_{A\alpha}$ knockout inhibits endocytosis at cerebellar synapses

(A, B) The SypH2X signal (mean + s.e.m.) induced by Train$_{20Hz}$ (A, black bar) and Train$_{40Hz}$ (B, black bar) in WT (4 experiments, black, left) and CaN$_{A\alpha}^{-/-}$ cerebellar boutons (8 experiments, red, middle). Data are also normalized and superimposed for comparison (right).

(C) Fluo2 fluorescence (F, left, au: arbitrary unit) and fractional changes (right, ΔF/F: fluorescence values divided by the baseline mean) in boutons induced by Train$_{20Hz}$ in wild-type (n = 13 experiments, each experiment includes 5-10 fluo2 spots, black, 4 mice) and CaN$_{A\alpha}^{-/-}$ cerebellar cultures (n = 9 experiments, red, 4 mice).

(D) Western blot of CaN$_{A\alpha}$, clathrin, dynamin, AP2, endophilin and actin (control) from wild-type and CaN$_{A\alpha}^{-/-}$ mouse brains.

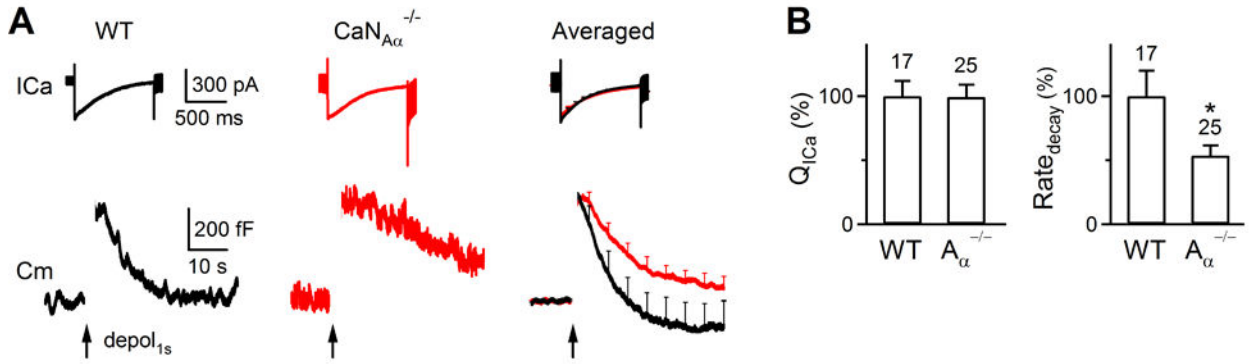

Figure 4. CaN$_{A\alpha}$ knockout inhibits endocytosis at chromaffin cells

(A) Sampled (left and middle) and averaged (right) ICa and Cm induced by 1 s depolarization in wild-type (17 cells, black) and CaN$_{A\alpha}^{-/-}$ chromaffin cells (25 cells, red). (B) QICa and Rate$_{decay}$ induced by 1 s depolarization in WT and CaN $_{A\alpha}^{-/-}$ chromaffin cells. *: $p<0.05$.